JP1.11 AMS Symposium on Observing and Understanding the
Variability of Water in Weather and Climate, 9-13 Feb. 2003, Long Beach, CA.

New Estimates of Continental Discharge and Oceanic Freshwater Transport

Aiguo Dai* and Kevin E. Trenberth
National Center for Atmospheric Research (NCAR)[$], Boulder, CO

Abstract

New estimates of freshwater discharge from continents were derived using stream-flow records from the world's largest 921 rivers, supplemented with estimates of discharge from unmonitored areas based on the ratios of runoff and drainage area between the unmonitored and monitored regions. The farthest downstream river-flow data were extrapolated to the river mouth using river transport model simulations forced by a runoff field. This new continental discharge estimate was then applied to estimate the meridional transport of freshwater within the oceans. The relatively new estimates of net water fluxes (*P-E*) over ocean surfaces derived from atmospheric moisture budget analyses based on the NCEP/NCAR and ECMWF reanalyses were used in the calculation of oceanic freshwater transport. Our results, which are improved in many aspects compared with previous estimates, show that global continental discharge is about 37288 $km^3\ yr^{-1}$ (1.2 *Sv*, 1 *Sv* = $1\times10^6\ m^3\ s^{-1}$) or about 35% of terrestrial precipitation. Compared with earlier indirect estimates of oceanic freshwater transport, our new estimates derived using the 921-river based discharge and the ECMWF reanalysis based *P-E* show improved agreement with available direct estimates for the Atlantic, Pacific, and Indian Ocean basins. The new estimates also show increased southward transports in the Atlantic Ocean and increased northward transports in the South Pacific Ocean.

1. Introduction

Estimates of continental freshwater discharge are needed for studying the global water cycle and freshwater budgets within the ocean. Baumgartner and Reichel (1975, BR75 hereafter) derived global maps of annual runoff and made estimates of annual freshwater discharge largely based on stream-flow data from the early 1960s analyzed by Marcinek (1964). Despite various limitations of the BR75 discharge data (e.g., rather limited station coverage, areal integration over 5^o latitude zones, no seasonal values), these estimates are still widely used in evaluations of ocean and climate models (Pardaens et al. 2002) and in estimating oceanic freshwater transport (Wijffels et al. 1992; Wijffels 2001), mainly because there have been few updated global estimates of continental discharge. The primary purpose of this study is to remedy this situation by providing estimates of monthly mean continental discharge for each $1^o\times1^o$ coastal box. The discharge results are discussed in detail in Dai and Trenberth (2003).

The relatively new estimates of net water flux (*P-E*) over ocean surfaces were derived from atmospheric moisture budget analyses based on the NCEP/NCAR and ECMWF reanalyses by Trenberth and Guillemot (1998) and Trenberth et al. (2001a). New *P-E* estimates will also be produced for the ERA-40 reanalyses that are underway. Although not problem-free, the *P-E* estimates as a residual of the atmospheric moisture budget (used in this study) are better than those based on model-predicted *E* and *P*, partly because atmospheric wind and moisture fields were calibrated every six hours by atmospheric sounding and satellite observations in the reanalyses.

On decadal and longer time scales, changes in soil and ground water are relatively small compared with the net water flux (*P-E*) over land. Therefore, the decadal mean fields of the *P-E* products over land may be used as proxies of terrestrial independent estimates. This provides additional evaluation of the *P-E* products.

* Corresponding author address: Aiguo Dai, NCAR/CGD, P.O.Box 3000, Boulder, CO 80307.
$ The National Center for Atmospheric Research is sponsored by the National Science Foundation.

The new continental discharge estimates and the oceanic *P-E* fields derived from the reanalyses, along with other estimates including those based on marine observations (Josey et al., 1998), are then used to derive meridional freshwater transport within each ocean basin and by the global oceans. Our goal is to update and improve the continental discharge estimates of BR75, provide an evaluation of the *P-E* fields from the reanalyses, and produce a detailed estimates of mean meridional freshwater transport by the oceans that can be used in climate and ocean model evaluations.

2. Data and Analysis Method

The monthly data sets used in this study are listed in Table 1. Through a tedious process we selected 921 ocean-reaching rivers from a merged global stream-flow data set that contains 8878 gauge stations (see Dai and Trenberth 2003 for details). The locations of the farthest downstream station for the 921 rivers are shown in Fig.1, together with a simulated network of the world's major river systems (by a river transport model or RTM described below). While the coasts in North and South Americas and Europe are well monitored, there are large river systems not monitored in tropical Africa and South Asia. Australia is a relatively dry continent and there is an absence of rivers along the southern coastline, so the network there appears to be sufficient.

Historical gauge records of stream-flow rates from the 921 stations were used to derive the long-term mean annual flow rate for the rivers and its standard deviation. The station mean flow rate were extrapolated onto the river mouth on the coast using the ratio between the simulated flow rates at the station and at the river mouth by the RTM forced by the annual runoff field from Fekete et al. (2000). The extrapolation to river mouth increases the river outflow substantially (e.g., by 25% for the Amazon river, see Table 2) and the global continental discharge by about 19% compared with unadjusted stream-flow from the farthest downstream stations, which are several hundreds to over one thousand km away from the river mouth for many large rivers.

The 921 rivers have a total drainage area of 79.5×10^6 km^2, which accounts for about 68% of the global non-ice, non-desert land areas. To estimate the discharge from the un-monitored areas, we made use of the ratio of runoff (based on Fekete et al. 2000) between un-monitored and monitored areas and discharged the un-monitored runoff at correct coastal locations using the STN-30p river network data base (Vörösmarty et al. 2000). The STN-30p was also used to derive the drainage area at the river mouth listed in Table 2.

The RTM used here was developed by M. L. Branstetter and J. S. Famiglietti and is described by Branstetter (2001) and Branstetter et al. (1999). The RTM is used in the NCAR Community Climate System Model (CCSM, Blackmon et al. 2001) for routing surface runoff into the ocean. Using a linear advection scheme at 0.5^o resolution, the RTM routes water from one cell to its downstream neighboring cell by considering the mass balance of horizontal water inflows and outflows. When forced with the Fekete et al. (2000) runoff fields, which were derived using a water balance model calibrated with stream-flow records from 663 stations, the RTM simulates the downstream river flow rates reasonably well (Table 2; also see Dai and Trenberth 2003).

The Fekete et al.(2000) runoff fields and the mean fields of *P-E* (Table 1) were used to drive the RTM. The simulated river outflows were used to derive freshwater discharge at each $1^o\times1^o$ coastal box, as implied by these runoff fields. These estimates of continental discharge were compared with that based on the 921 rivers.

Current estimates of net water flux over the ocean surfaces (e.g., da Silva et al. 1994; Josey et al. 1998) still have large uncertainties, as direct measurements of precipitation and reliable estimates of surface evaporation have been unavailable over most oceans. As an alternative, here we used the oceanic *P-E* fluxes derived from atmospheric moisture budget analyses (Table 1), along with other estimates including those based on marine observations (Josey et al. 1998), in deriving estimates of meridional transport of freshwater by the oceans.

Table 1: Data sets used in this study. All are monthly.

Variables	Type & coverage	Resolution	Period	Source & Reference
Streamflow	station, land		1-100+ yrs	NCAR, Bodo 2001
Runoff	composite, land	0.5°	climatology	GRDC/UNH, Fekete et al. 2000
E-P	NCEP/NCAR re-analysis, global	2.8°	1979-1995	NCAR, Trenberth & Guillemot 1998
E-P	ECMWF reanalysis	2.8°	1979-1993	NCAR, Trenberth et al. 2001a
E-P, E	sfc. observations, ocean only	1.0°	1980-1993	SOC, Josey et al. (1998)
P	gauge + satellite + reanalysis, global	2.5°	1979-1998	CMAP, Xie & Arkin 1997
P	gauge + satellite, global	2.5°	1979-1999	GPCP, Huffman et al. 1997
T	station data, land	0.5°	1961-1990	CRU, New et al. 2000
River basin Attributes	simulated river network STN-30p	0.5°		UNH, Vörösmarty et al. 2000

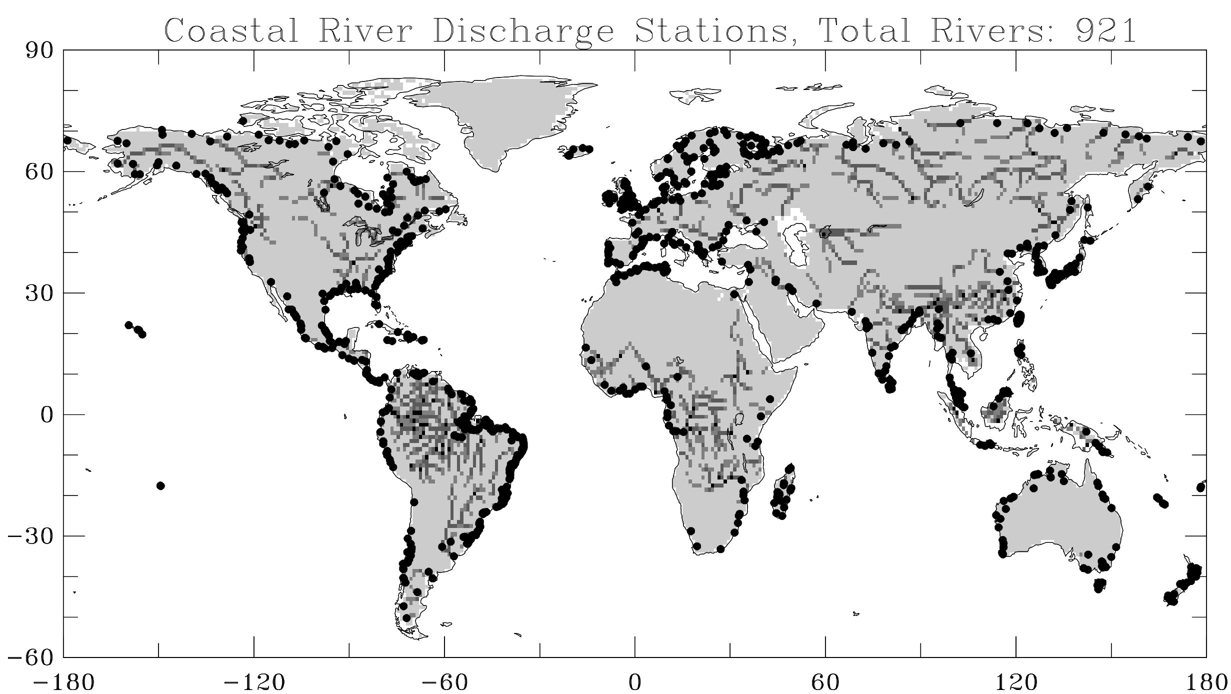

Fig.1: Distribution of the farthest downstream stations for world largest 921 rivers included in these studies. Also shown are the worlds major river systems simulated by a river transport model.

Table 2: World's largest 50 rivers (by the estimated river mouth flow rate *Vol*). Listed are long-term mean station (*Stn*, ± standard deviation *s.d.*) and river transport model (*RTM*) simulated river flow (in km^3 yr^{-1}) at the station location, and the estimated annual volume (*Vol*) and drainage area (*D.A.*, based on STN-30p, in 10^3 km^2) at the river mouth. The composite annual runoff data of Fekete et al.(2000) were used in the RTM simulation. *nyr* is station record length in years, *lon* and *lat* are longitude and latitude for the station.

No	Name	*Vol* at Station		River Mouth		Stn	*nyr*	*lon*	*lat*	Station, Country
		Stn±s.d.	*RTM*	*Vol*	*D.A.*	*D.A.*				
1	Amazon	5330±426	5083	6642	5854	4619	49	-55.5	-2.0	Obidos, Brazil
2	Congo	1271±130	1266	1308	3699	3475	81	15.3	-4.3	Kinshasa, Congo
3	Orinoco	984±112	1141	1129	1039	836	66	-63.6	8.1	Pte Angostu, Venezuela
4	Changjiang	910±133	996	944	1794	1705	49	117.6	30.8	Datong, China
5	Brahmaputra	613± 51	617	628	583	555	6	89.7	25.2	Bahadurabad,Bangladesh
6	Mississippi	536±130	458	610	3203	2896	71	-90.9	32.3	Vicksburg, USA
7	Yenisey	577± 42	525	599	2582	2440	60	86.5	67.4	Igarka, Russia
8	Paraná	476± 96	589	568	2661	2346	89	-60.7	-32.7	Timbues, Argentina
9	Lena	526± 63	456	531	2418	2430	60	127.4	70.7	Kusur, Russia
10	Mekong	292± 33	271	525	774	545	7	105.8	15.1	Pakse, Laos
11	Tocantins	356± 64	398	511	769	742	20	-49.7	-3.8	Tucurui, Brazil
12	Tapajos	337± 32	545	415	502	387	24	-56.8	-5.2	Jatoba, Brazil
13	Ob	397± 61	433	412	2570	2430	65	66.6	66.6	Salekhard, Russia
14	Ganges	382± 76	428	404	956	952	21	88.1	24.5	Farakka, India
15	Irrawaddy	258± 29	324	393	406	118	11	96.0	21.9	Sagaing, Myanmar(Burm
16	St Lawrence	226± 26	318	363	1267	774	64	-74.7	45.0	Cornwall ON, USA
17	Amur	312± 60	359	354	2903	1730	54	137.0	50.5	Komsomolsk, Russia
18	Xingu	272± 44	325	302	497	446	26	-52.2	-3.2	Altamira, Brazil
19	Mackenzie	288± 29	260	290	1713	1660	21	-133.7	67.5	Arctic Red, Canada
20	Xijiang	221± 45	179	270	409	330	46	111.3	23.5	Wuzhou, China
21	Columbia	172± 33	194	252	724	614	121	-121.2	45.6	The Dalles, USA
22	Magdalena	231± 35	175	231	252	257	19	-74.9	10.2	Calamar, Colombia
23	Uruguay	165± 54	65	228	356	249	12	-58.0	-31.4	Concordia, Argentina
24	Yukon	203± 18	203	212	852	831	21	-162.9	61.9	Pilot Stn, Alaska
25	Atrato	56± 7	33	204	34	9	24	-76.7	6.2	Tagachi, Colombia
26	Danube	202± 36	166	202	788	807	80	28.7	45.2	Ceatal Izma, Romania
27	Niger	33± 9	102	193	2240	1516	29	3.5	11.9	Gaya, Niger
28	Ogooué	148± 22	139	186	210	204	42	10.2	-0.7	Lambaréné, Gabon
29	Essequibo	69± 15	25	154	151	67	13	-58.6	5.8	Plantain Is, Guyana
30	Fraser	86± 11	121	144	245	217	79	-121.4	49.4	Hope, Canada
31	Pechora	135± 16	126	140	302	312	36	52.2	67.6	Oksino, Russia
32	Nelson	70± 17	84	126	1047	997	34	-97.9	54.8	u/s Bladder, Canada
33	Khatanga	78± 3	69	124	371	275	13	102.5	72.0	Khatanga, Russia
34	Sepik	119± 9	112	123	77	41	4	142.2	-4.2	Ambunti, Papua New Gu
35	Kolyma	99± 26	83	118	666	526	17	158.7	68.7	Kolymskoye, Russia
36	Zambeze	105± 44	404	117	1989	940	4	33.6	-16.1	Matundo-Cai,Mozambique
37	Severnaya Dv	106± 20	176	112	367	348	112	41.9	64.1	Ust Pinega, Russia
38	Indus	89± 25	125	104	1143	975	31	68.3	25.4	Kotri, Pakistan
39	Sanaga	63± 9	65	99	129	132	37	10.1	3.8	Edéa, Cameroon
40	Godavari	97± 32	86	97	312	299	74	81.8	16.9	Polavaram, India
41	Rajang	70± 10	83	93	56	34	32	112.9	2.0	Kapit Wharf, Malaysia
42	Sao Francisco	89± 28	127	90	615	623	56	-37.0	-10.0	Traipu, Brazil
43	Usumacinta	59± 12	57	89	68	51	35	-91.5	17.4	Boca del Ce, Mexico
44	Maroni	59± 14	11	86	65	64	4	-54.5	5.0	Langa Tabbe, Surinam
45	Rhine	73± 14	86	75	165	180	6	6.1	51.8	Lobith, Netherlands
46	Purari	74± 13	60	74	34	29	6	145.1	-7.0	Wabo Dam, Papua New Gu
47	Caniapiscau	43± 13	11	73	143	87	31	-69.2	57.4	Chute de la, Canada
48	Mahanadi	60± 33	63	73	141	132	6	84.0	20.8	Kaimundi, India
49	Sacramento	21± 7	11	69	193	61	31	-121.5	38.6	Sacramento, USA
50	Jacui	55± 11	50	69	81	71	5	-51.5	-30.0	Passo do Ra, Brazil
	Total:	17492±552#	18079	21152	50415	42364				

\# This number, which was estimated as the square root of the sum of the variance of the listed rivers, provides only an estimate for the true s.d. of the total volume.

3. Results

3.1 Freshwater Discharge from World's Major Rivers

Table 2 shows the annual mean river flow rate and drainage area at the farthest downstream station and the river mouth for the world's largest 50 rivers (the list extends to top 200 rivers in Dai and Trenberth 2003). Table 2 shows that the farthest-downstream station data underestimate, by 10 to over 100%, the river discharge and drainage area at the river mouth in many cases (e.g., Amazon, Orinoco, Mississippi, Paraná, Mekong, Irrawaddy, St Lawrence, and Niger). Most earlier estimates of stream-flow and drainage area for the world's largest rivers used unadjusted data from the available farthest downstream station (e.g., Probst and Tardy 1987; Perry et al. 1996; Grabs et al. 1996, 2000). These unadjusted estimates not only underestimate the true river outflow, but also contribute to the large range among various estimates of flow rate for world's major rivers because the distance from the farthest downstream station to the river mouth varies among different studies from hundreds to thousands of kilometers (Perry et al. 1996). For example, Perry et al. (1996) listed the Amazon with a mean flow rate of 6088±465 (s.d.) km^3 yr^{-1} based on 11 different sources, whereas it is 6000 km^3 yr^{-1} in BR75. Although these are higher than our mean flow rate (5330 km^3 yr^{-1}) at station Obidos, they are about 10% lower than our estimate of Amazon mouth flow (6642 km^3 yr^{-1}).

The world's 50 largest rivers (Table 2) account for ~57% of the global discharge, whereas their total drainage area is ~43% of the global actively drained land areas (i.e., excluding glaciers and deserts). Adding the next 150 largest rivers (Table A in Dai and Trenberth 2003) increases these to 67% and 65%, respectively, while adding the next 721 rivers in our data set of coastal stations changes the numbers only moderately (to 73% and 68%, respectively). This suggests that an increasingly large number (in thousands) of smaller rivers are needed to improve the coverage of the station network for monitoring global freshwater discharge.

The total global freshwater discharge, excluding that from Antarctica, is about 37288 ± 662 km^3 yr^{-1} (Table 3), which is ~7.6% of global precipitation or 35% of terrestrial precipitation (excluding Antarctica and Greenland) based the averaged precipitation of CMAP and GPCP (cf. Table 1). Since a time series of global discharge is hard to derive because of a changing number of gauges, this uncertainty range was estimated as the square root of the sum of the variance of long-term mean annual flows at the farthest downstream stations of all the 921 rivers multiplied by 1.187, the global-mean factor for converting the farthest downstream station flows to the river mouth outflows. Hence it is based on the assumption that the covariance of stream-flow among large rivers is small.

The stream-flow of many rivers has a large annual cycle. Fig. 2 compares the mean annual cycle of discharge (thick-solid curve) with those of basin-integrated precipitation (thin-solid curve), runoff and *P-E* for the 10 largest rivers. Note that the RTM is not used in the basin-wide summation and therefore the differences between the river discharge and the basin-integrated values illustrate the effects of snow and the time delay of water traveling upstream to the river mouth. The Amazon has the highest flow from May to June, while its basin-integrated precipitation, runoff, and *P-E* peak in early spring. This lag reflects the time needed for surface runoff to travel to the river mouth. For the Changjiang, Brahmaputra/Ganges, Mississippi, Mekong, and smaller rivers, this time lag is shorter (about one month or less), suggesting that the seasonal changes in surface runoff occur in the area not far away from the river mouth. The Congo and Paraná have relatively small annual cycles, even though precipitation and runoff (for Paraná only) exhibit large seasonal variations.

The big Russian rivers (Yenisey, Lena, Ob, etc.) have large peak flows in June, which result from spring (April-May) snowmelt as precipitation does not peak until July-August in these regions (Fig. 2). In fact, the drainage area-integrated discharge and precipitation for the entire Arctic region (Dai and Trenberth 2003; Grabs et al. 2000) are very similar to those for Yenisey and Lena. Early-spring snowmelt over the Mississippi basin also appears to be the main reason for the April peak discharge from the Mississippi, whose integrated precipitation peaks in May-June.

At low latitudes, the basin-integrated *P-E* generally agrees with the Fekete et al. runoff, indicating that the monthly *P-E* fields are reasonable proxies of monthly runoff provided the areas are large enough. One exception is the ECMWF *P-E* over the Congo River basin, where it follows the precipitation annual cycle rather than the runoff (Fig. 2). This bias is reflected in the high values of *P-E* in tropical Africa and is mainly due to the higher-than-observed precipitation in the ECMWF data resulting from the spurious ITCZ shift over Africa (Trenberth et al. 2001b).

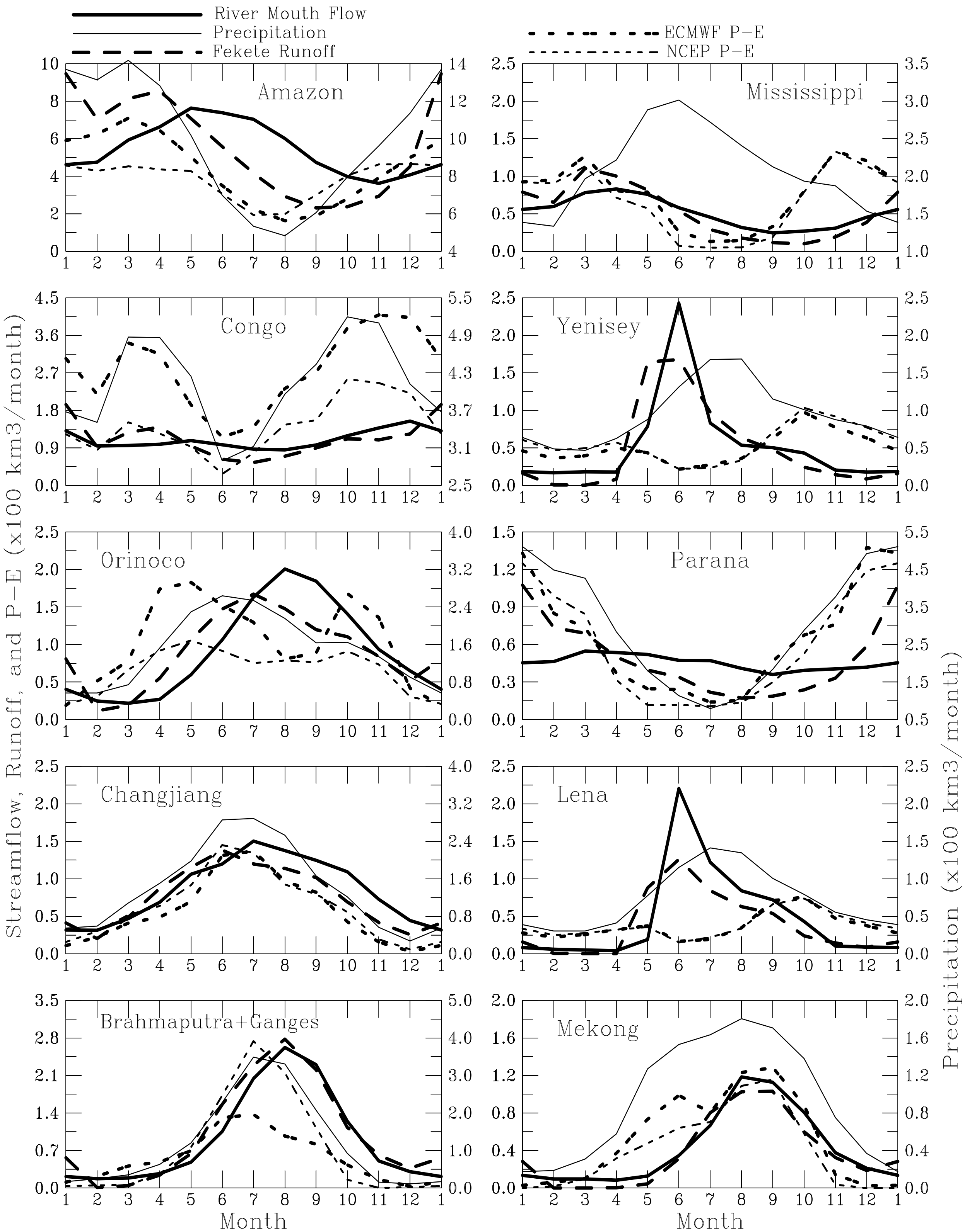

Fig.2: Mean annual cycle of river discharge, river-basin integrated precipitation (read on the right ordinate), runoff, and reanalysis P-E for world largest 10 rivers. Note that the RTM was not used for this plot

3.2 Total Freshwater Discharge into the Ocean Basins

Table 3 compares our estimates of total freshwater discharge into the ocean basins with four earlier estimates. Discharge from groundwater, which was estimated to be around 5% of the total discharge by Lvovich (1970), is included only in the estimates using the *P-E* data and from Korzun (1977). Small surface freshwater discharge from Antarctica (=1987 km^3 yr^{-1} according to BR75) and changes in land storage (e.g., effects of melting glaciers) are also not included. Our 921-river-based estimate of the global discharge is 37288±662 km^3 yr^{-1} (1 km^3 yr^{-1} = 31.69 m^3 s^{-1}), which is very close to that of BR75 (37713) and Perry et al. (1996)(37768). However, Perry et al. (1996) used stream-flow rates from the farthest downstream stations, which underestimate the true river discharge by an average of 18.7% in our analysis (see Tables 2). This result implies that the power law size distribution used by Perry et al. (1996) substantially overestimates the total discharge from small rivers with an annual flow rate <250 m^3 s^{-1}.

The global discharge implied by the Fekete et al. runoff and ECMWF *P-E* is only slightly higher than that based on stream-flow data, while the NCEP *P-E* results in lower global discharge (Table 3), consistent with its dry bias (Dai and Trenberth 2003). This result suggests that the ECMWF ERA-15 *P-E* is likely to be more reliable over global land than the NCEP *P-E* and it may be considered as a proxy for terrestrial runoff for estimating continental discharge, although problems exist in Africa and South America. Although the various estimates of total continental discharge listed in Table 3 are in good agreement, except for Korzun (1977), their partitioning of the total discharge into individual ocean basins differs substantially. For example, compared with the 921-river-based estimates, the discharge implied by the Fekete et al. runoff is lower for the Arctic and Atlantic Oceans and higher for the Pacific and Indian Oceans and the Mediterranean and Black Seas, whereas

Table 3: Comparison of estimates of mean annual continental freshwater discharge into the individual and global ocean (km3 yr^{-1}).

	Arctic	Atlantic	Indian	Med.Sea	Pacific	Total
Largest 921 Rivers	3658	19168	4532	838	9092	37288
Fekete Runoff	3263	18594	5393	1173	10420	38843
ECMWF P-E	3967	20585	4989	1144	7741	38426
NCEP/NCAR P-E	4358	16823	3162	909	7388	32640
Fekete et al.(2000)	2947	18357	4802	1169	11127	38402
Korzun (1977)	5220	20760	6150	-	14800	46930
Baumgartner & Reichel (1975)	2600	19300	5600	-	12200	37713
Oki (1999)	4500	21500	4000	-	10000	40000

Largest 921 Rivers: scaled up by accounting for the unmonitored areas and the runoff ratio at 4° latitude resolution.
Korzun (1977): includes ground-water runoff (2200 km3 yr^{-1} globally) and iceberg runoff (2700 km3/yr globally).
Med.Sea: includes the Mediterranean and Black Seas.
Total: excludes discharge into inland (besides Black) seas and from Antarctica.

the ECMWF *P-E* implies higher discharge into all but the Pacific basin. Table 4 shows that both of the reanalysis *P-E* fields underestimate the discharge into the Pacific Ocean significantly -- by 15% for ECMWF and 19% for NCEP compared with the river-based estimate. These biases result primarily from the smaller *P-E* than the Fekete et al. runoff over China and Southeast Asia (Dai and Trenberth 2003).

For the Arctic Ocean, the estimates range from 2600 $km^3\ yr^{-1}$ by BR75 to 5220 $km^3\ yr^{-1}$ by Korzun (1977). Grabs et al. (2000) obtained an annual discharge of 2603 km^3 into the Arctic Ocean by totaling discharge data from 35 farthest downstream stations, which account for 70% of the total Arctic drainage area. Assuming the un-monitored 30% drainage area has similar runoff rates, this would imply a total discharge of 3718 $km^3\ yr^{-1}$, which is comparable to our estimates (except for the NCEP case) (Table 3).

Fig. 3 shows that the right amount of total discharge into a particular ocean basin may result from discharges coming off wrong coasts. For example, the total discharge from the western and eastern coasts of the Indian Ocean is similar for the 921-river and NCEP cases, but the NCEP *P-E* implies too much runoff from Australia and too little from Africa.

3.3 Geographical Distribution of Discharge into the Oceans

Fig.3 shows four estimates of annual freshwater discharge rates from individual 4^o lat × 5^o lon coastal boxes. Also shown is the total discharge (in $10^3\ m^3\ s^{-1}$) from the coasts behind the solid lines. These estimates were derived using long-term mean stream-flow data from the 921 rivers (using extrapolated river mouth flow and accounting for the discharge from the un-monitored areas), the composite annual runoff from Fekete et al. (2000), and the multi-year averaged *P-E* fields derived from the reanalyses (see Table 1).

As indicated by the scale of the color bar, coastal discharge rates vary from <10 to 215,000 (at the Amazon mouth) $m^3\ s^{-1}$ per $4^o \times 5^o$ box. Most of the global discharge comes from the world's major rivers, whose mouths are indicated by the boxes in warm colors in Fig. 3a. The eastern coasts of the Americas, primarily in the Tropics, provide ~40% of global discharge (Fig.3a). Discharge from East Asia into the North Pacific accounts for another ~15% of the total. However, less than 10% of the global discharge comes from the western coast of South America.

The integrated coastal discharge provides an easier measure (than the colors) for comparison among the four cases. It can be seen that the Fekete et al. runoff implies discharges comparable to the river-based estimates from most of the coastlines except for those from East Asia (too low), Indonesia, the Bay of Bengal and tropical West Pacific Islands (too high) (Fig.3b). The ECMWF *P-E* implied discharges are also similar to the river-based estimates, except for the coasts of East Asia, western Australia, and Africa (Fig. 3d). The NCEP case reproduces the discharge into the Arctic, South Atlantic, and South Pacific Ocean, but has large deficiencies over eastern Africa, Europe, and East Asia (Fig. 3c). In general, both the ECMWF and NCEP cases underestimate discharges from northern Africa and East Asia, largely due to the negative values of *P-E* (which was set to zero in the RTM simulations) over these regions (Dai and Trenberth 2003).

Fig. 4 shows the annual mean continental freshwater discharge into the global oceans for each 1^o latitude zone (stepwise lines) and the discharge accumulated starting from 90^oN (upper curves). For comparison, the estimate by BR75 is also shown (thick-solid line). As expected, the continental discharge is dominated by the peak outflows from the world's largest rivers such as the Amazon (~0.21 *Sv* at 0.75^oS, 1 $Sv = 10^6\ m^3\ s^{-1}$), Congo (0.041 *Sv* at 5.75^oS), Orinoco (0.036 *Sv* at 9.25^oN), Changjiang (0.030 *Sv* at 32.25^oN), Brahmaputra/Ganges (0.033 *Sv* at 24.25^oN), Mississippi (0.019 *Sv* at 30.25^oN), and Paraná (0.018 *Sv* at 34.75^oS) (note that the peaks in Fig. 4 may exceed these numbers because of contributions from small rivers within the same latitude band). The northern mid- to high-latitudes (45-75^oN) encompass the largest landmass and many large rivers, including the Yenisey, Lena, Ob, Amur in Russia, Mackenzie and St. Lawrence in Canada, and Yukon in Alaska. Many of the Russian and Canadian rivers run from south to north and enter the Arctic Ocean. Collectively, these rivers provide a large freshwater discharge into the Arctic, North Atlantic and North Pacific Oceans, thereby affecting the oceanic water budget and circulation, both locally and globally, especially through the thermohaline circulation. Since the Northern mid- and high-latitudes are expected to have the largest temperature and precipitation increases in the next 100-200 years due to increases in CO_2 and other greenhouse gases (e.g., Dai et al. 2001a,b), it is vital to establish an observed baseline.

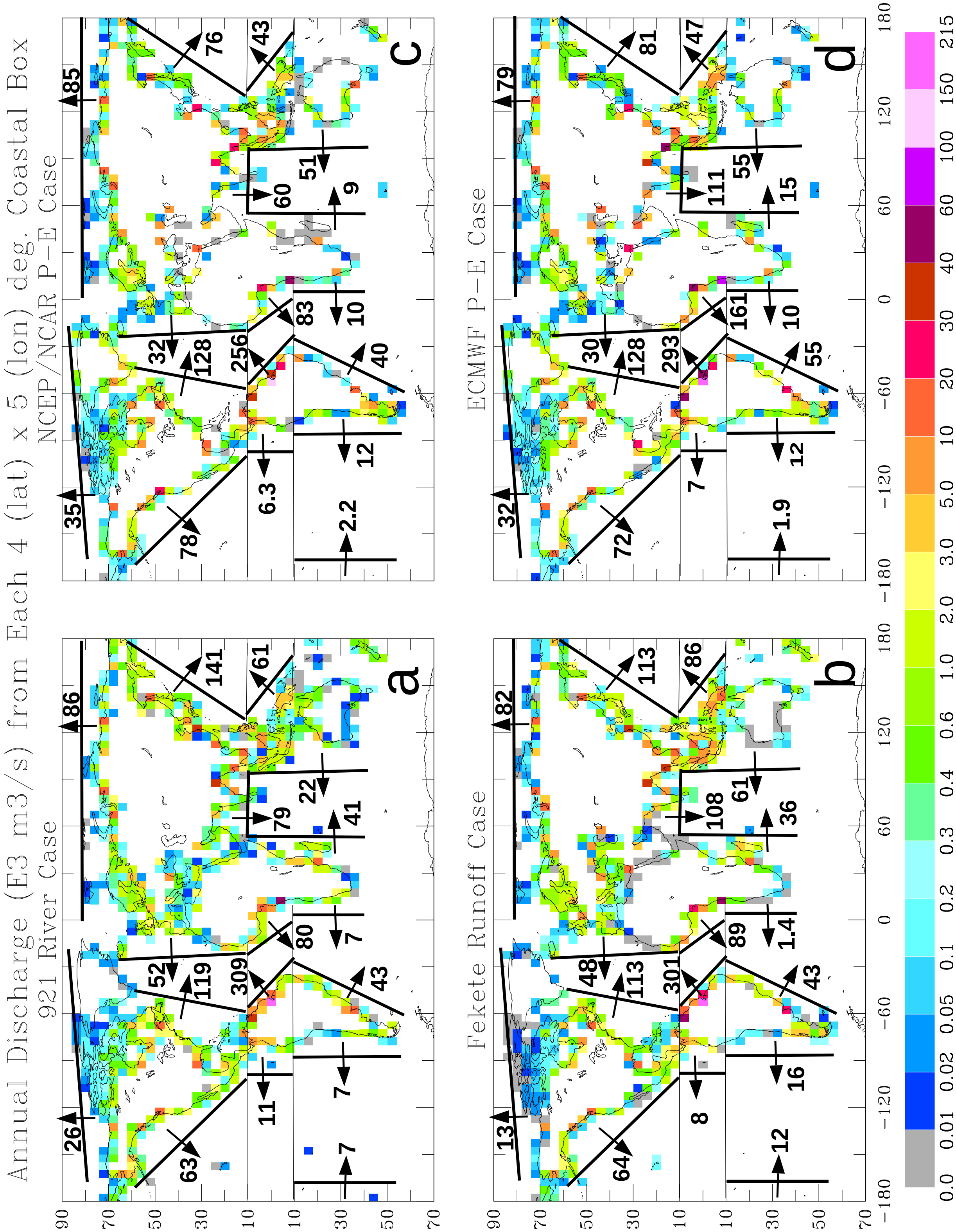

Fig.3: Annual discharge rate (10^3 m^3 s^{-1}) from each 4^o lat by 5^o lon coastal box. The numbers are the total discharge (in 10^3 m^3 s^{-1}) from the coasts behind the solid lines. Blank coastal boxes have zero discharge.

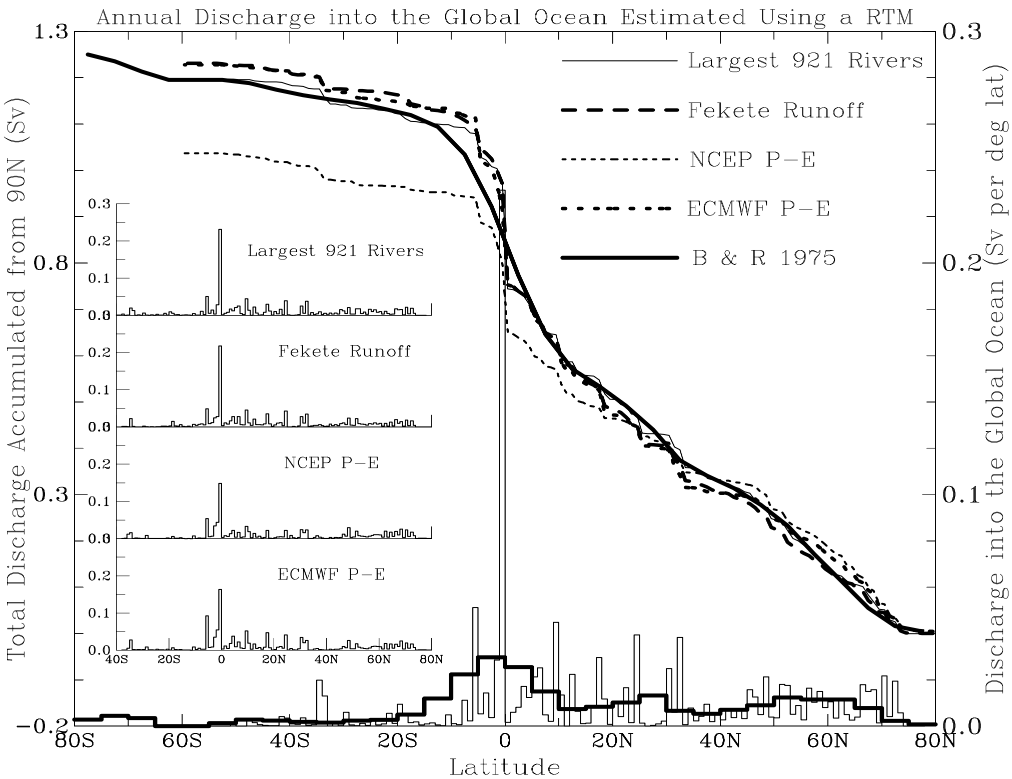

Fig.4: Estimates of annual mean continental freshwater discharge into the global oceans for each 1^o latitude zone (right ordinate and lower stepwise lines, and the insert) and the cumulated discharge starting from 90^{o}N (upper curves). Each line pattern represents an estimate based either on the largest 921 rivers (thin solid line) or on a runoff field (dashed lines), which was used to force a river transport model to derive the discharge. Also shown is an estimate from Baumgartner and Reichel (1975, thick solid line).

The RTM reproduces the peak outflows from the world's largest rivers when forced with the Fekete et al. runoff and the reanalysis *P-E* fields, although the magnitude of the peaks differ somewhat from the estimates based on observations (see the insert of Fig.4, also see Table 2). These differences are also shown by the accumulated discharges. Note that the accumulated discharge, a common measure used in previous studies (e.g.,Wijffels 2001), integrates the errors from the 90^{o}N southward, and the differences at southern latitudes do not reflect the actual errors at those latitudes because contributions are small south of 10^{o}S.

The accumulated discharge for the NCEP *P-E* case is considerably lower than the others, whereas the BR75 case agrees remarkably well with our estimates based on the stream-flow data, Fekete et al. runoff and ECMWF *P-E*. However, the latitudinal distribution from BR75 at 5^o resolution is too smooth and quite unrealistic. Even after smoothing the 1^o discharge data using 5^o lat running-mean, large differences still exist between the BR75 and our estimates, whereas the agreement among our four different estimates improves (Dai and Trenberth 2003).

3.4 Seasonal Cycle of Continental Discharge

Fig.5 shows the mean annual cycle of total freshwater discharge into the individual and global oceans, as estimated based on the 921 rivers with and without scaling for the contribution from the unmonitored areas, Fekete et al. runoff, and *P-E* fields from the NCEP and ECMWF reanalyses. The inclusion of the unscaled gauge-based estimate shows that the contribution from the unmonitored areas does not significantly alter the phase of the mean annual cycle and is large, ranging from ~20% of the monitored discharge for the Atlantic to ~100% for the Pacific.

The discharge into the Arctic Ocean has a sharp peak in June arising from snow-melt in late spring, although the Fekete et al. result has a lower maximum but with higher values in most other months. Both the NCEP and

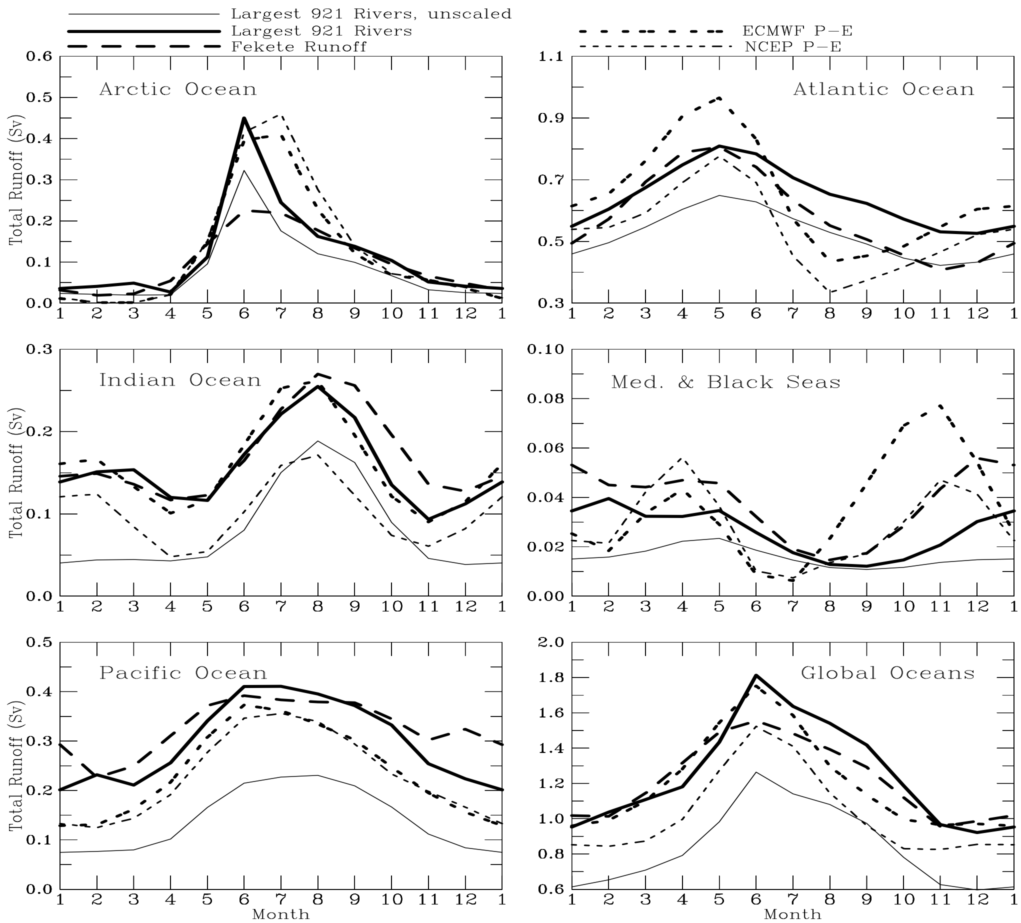

Fig.5: Mean annual cycle of freshwater discharge into individual and global oceans based on various estimates. The thin solid line is for the estimate based on the 921 rivers without scaling to account for the un-monitored areas.

ECMWF *P-E* fields result in too much discharge in July and too little from January to March. We tested various combinations of k and t_S in the simple snow model (see Dai and Trenberth 2003) to account for snowmelt but all produced the peak discharge in July. This suggests that the simple scheme has limitations, probably arising from the use of only daily mean temperatures.

The total freshwater discharge into the Atlantic Ocean has a similar peak in May for all but the ECMWF and the unscaled cases (Fig. 5). For the Atlantic, the ECMWF case has too much discharge in May and too low discharge in August and September and the latter bias is even larger for the NCEP case. The May peak in all the cases results from the concurrence of high discharge in May from the Amazon and Mississippi (Fig.2). The discharge into the Indian Ocean peaks in August, mainly from the heavy Indian summer monsoon rainfall. For the Pacific Ocean, the discharge peaks about June-July primarily because of heavy monsoon rainfall over East Asia during these months. Over the Mediterranean and Black Seas, the discharge is low in the warm season and high during winter and spring seasons. Globally, total freshwater discharge is high from May to September with a peak in June and lull from October to April. This annual cycle results mainly from the discharge from Northern Hemisphere land areas. All the cases broadly reproduce the annual cycles revealed by the gauge data.

3.5 Freshwater Transport by the Oceans

Fig.6 compares various estimates of northward freshwater transport by the global oceans. Using the 921-river based discharge, the various oceanic *P-E* fields result in large differences in the oceanic freshwater transport. In particular, the Southampton Oceanographic Centre (SOC) *P-E* product (Josey et al. 1998), which was derived based on marine observations, and the mean precipitation (of GPCP and CMAP, see Table 1) minus SOC *E* case produce essentially all southward transport at all latitudes, which is physically unrealistic. The *P-E* fields derived from the ECMWF and NCEP reanalyses (see Table 1) result in similar transports at most latitudes. These transports are generally lower than those of Wijffels et al. (1992)and the inferred oceanic transports by the atmospheric moisture transport in the reanalyses. This is especially true around 5-10^{o}S and south of 35^{o}S. As a result, these estimates have a small (≤0.15 *Sv* for the ECMWF case and ≤0.31 *Sv* for the NCEP case) southward transport south of 70^{o}S, where oceanic transports should approach zero. These biases, which represent the accumulated errors in deriving the transport starting from the North Pole, result from the imbalances between the 921-river based continental discharge and the reanalysis based oceanic *P-E* fields.

The oceanic transports inferred from atmospheric moisture transports (i.e., the reverse of atmospheric transports) have the desired feature of zero transports at the poles. However, they can differ substantially from the actual oceanic freshwater transport at many latitudes because a number of large rivers, such as the Mississippi, Orinoco, Paraná, Congo, and Amazon, transport terrestrial runoff to a large distance in the north-south direction. This meridional transport of freshwater by rivers is largest in low latitudes. It should result in and is probably responsible for the substantial differences between the ECMWF and NCEP *P-E* cases and the inferred transports in low latitudes Fig.6).

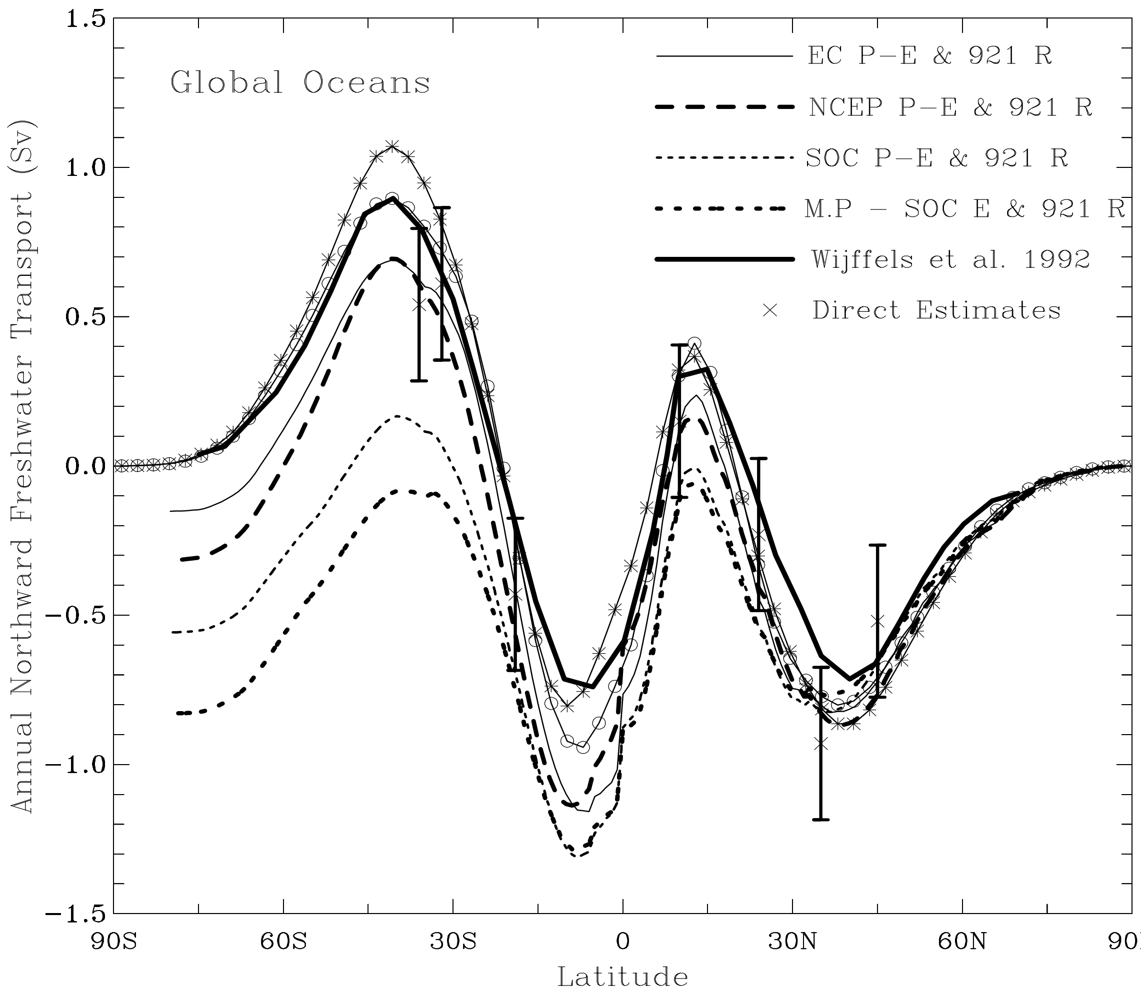

Fig.6: Latitudinal distribution of annual freshwater transport (positive northward) by the global oceans estimated using various oceanic *P-E* (see text for more details) and continental runoff estimated based on streamflow data of world largest 921 rivers. The thin-solid line with circles and stars are inferred oceanic transport of freshwater from atmospheric moisture transport in the ECMWF and NCEP/NCAR reanalyses, respectively. The thick solid line is an estimate by Wijffels et al. (1992) based on BR75. Also shown are some direct estimates (crosses) adopted from Wijffels (2001).

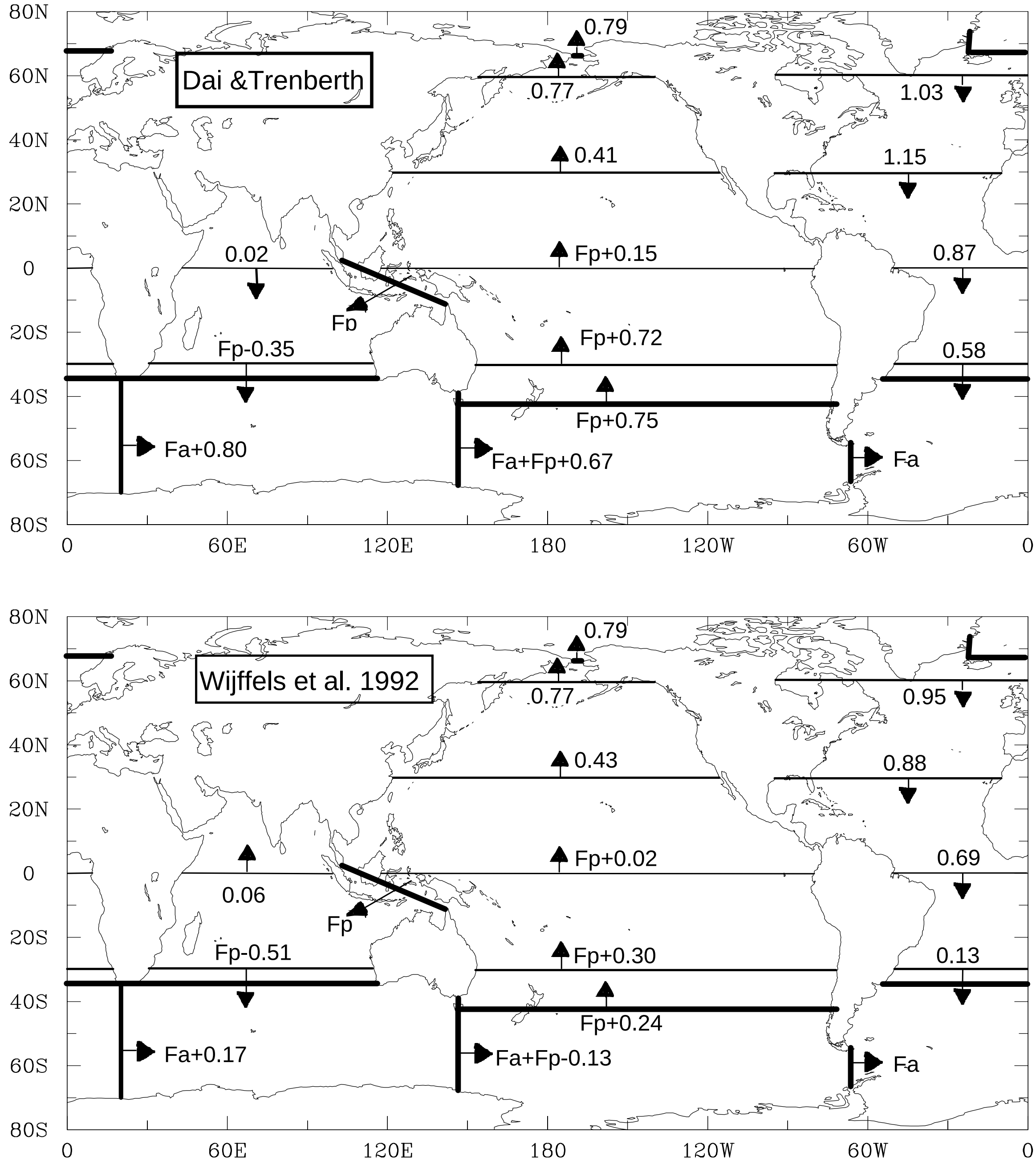

Fig.7: *Top*: Oceanic freshwater flux at selected latitudes estimated by this study using the 921-river based discharge and the ECMWF reanalysis based oceanic *P-E* (Table 1). The solid lines are ocean basin boundaries. *Bottom*: Same as *Top* but from Wijffels et al. (1992).

The Wijffels et al.(1992) estimate (thick solid line in Fig. 6), which was largely based on discharge and other data from BR75, has unbiased transports at the poles. It is considerably higher than the reanalysis *P-E* cases at most latitudes, especially within 0-15^{o}S where the BR75 discharge data have considerably errors (cf. Fig. 4). The available direct estimates have large uncertainties, which make comparisons inconclusive. Nevertheless, our estimates based on the reanalysis *P-E* (especially the ECMWF case) and the 921-river based discharge yield better agreement with the seven direct estimates despite their negative biases at the South Pole (Fig. 6).

Fig.7 compares the oceanic freshwater fluxes at selected latitudes estimated by this study (based on the ECMWF *P-E* and 921-river based discharge) and by Wijffels et al. (1992). In both cases, the transport at the

Bering Strait was assigned a value of 0.79 *Sv* based on observations (see Wijffels et al. 1992), and the integration starts from the Arctic Ocean to the North and the South Atlantic Oceans. Current estimates of the Indonesia Throughflow (F_P) are very uncertain, probably in the range of 5-10 *Sv* (Wijffels 2001). It can be seen that our estimated southward transports in the Atlantic Ocean and northward transports in the South Pacific Ocean are considerably higher than those of Wijffels et al.(1992). Furthermore, our eastward transports by the Antarctic Circumpolar Currents (ACC) are higher than those of Wijffels et al. (1992) at most longitudes.

Comparisons with available direct, basin-wide estimates of oceanic transports (Figs. 8-10) seem to suggest that our estimate (based on the ECMWF *P-E* and 921-river based discharge) is generally closer to those *in-situ* data based direct estimates than Wijffels et al. (1992) is. This is especially true at southern latitudes of the Atlantic, Pacific and Indian Oceans. Because of this and the errors in the BR75 discharge, we believe our estimate for the ECMWF *P-E* case is likely to be more reliable than that of Wijffels et al. (1992) and the inferred global transports (Fig. 6) at most latitudes (north of ~50^{o}S).

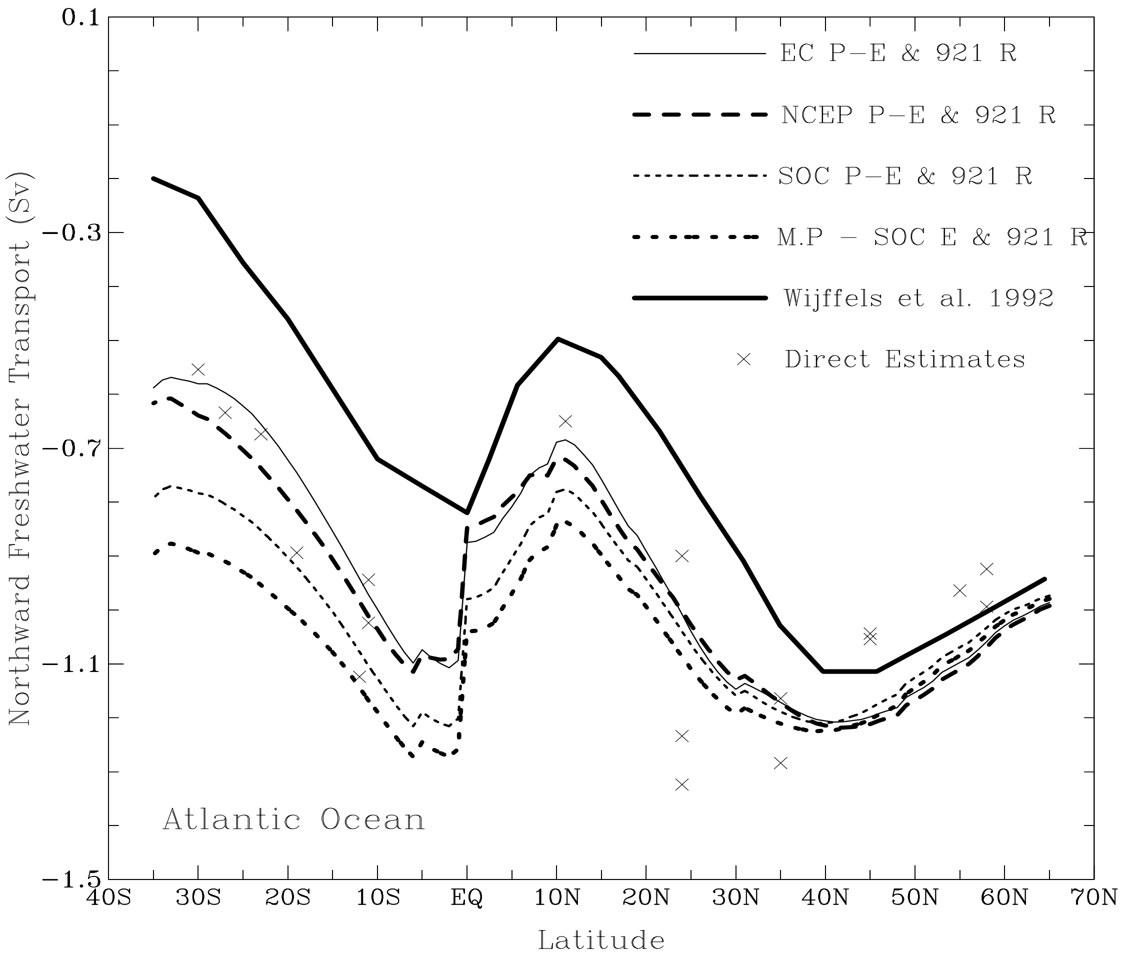

Fig.8: Same as Fig. 6 but for the Atlantic Ocean.

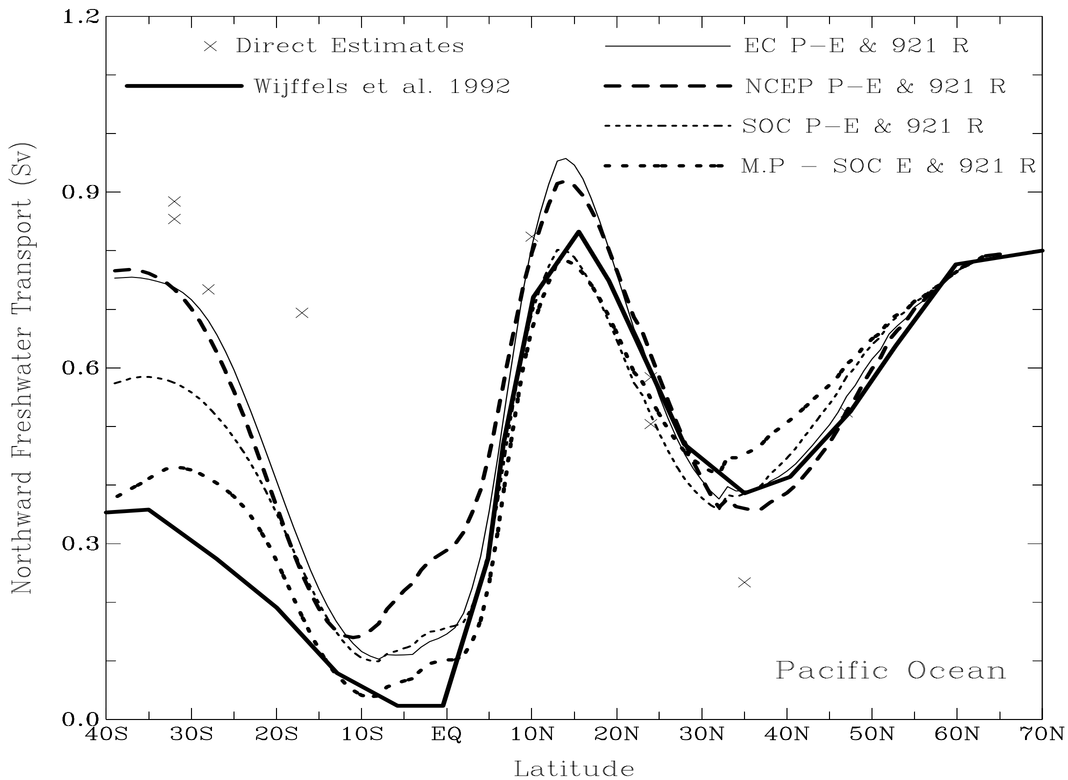

Fig.9: Same as Fig.6 but for the Pacific Ocean, with the Indonesia Throughflow excluded

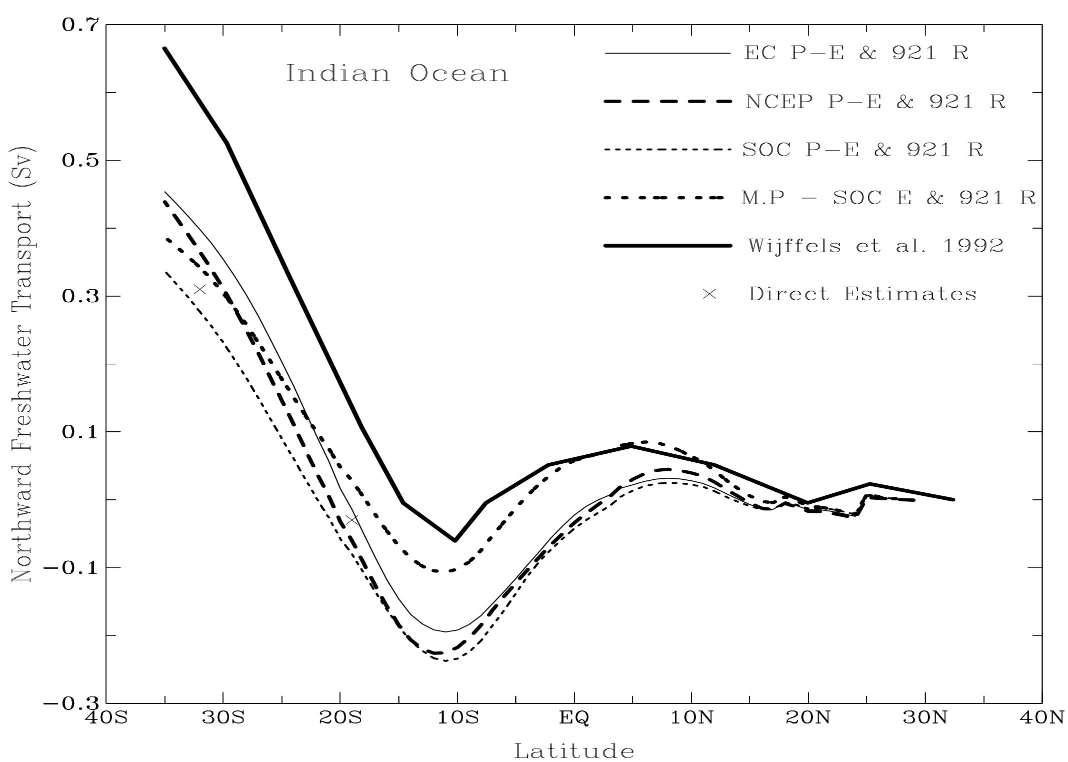

Fig.10: Same as Fig.9 but for the Indian Ocean, with only two direct estimates at 19^{o}S and 32^{o}S.

4. Summary

We have created and compared several estimates of continental freshwater discharge into the oceans. The first is built on discharge data from 921 ocean-reaching rivers selected from several comprehensive stream-flow data sets. The drainage area of the 921 rivers is 79.5×10^6 km^2, or about 68% of global non-ice, non-desert land areas. We estimated the river mouth outflow from the world's large rivers by adjusting the stream-flow rate at the farthest downstream station using the ratio of simulated flow rates (or drainage areas in some cases) at the river mouth and the station. The discharge from the un-monitored areas was estimated based on the ratios of runoff and drainage area between the un-monitored and monitored areas at each latitude. A river transport model, the composite runoff field from Fekete et al. (2000), and a simulated global river data base STN-30p were used in this analysis. Long-term mean annual and monthly freshwater discharge at each latitude into individual and global oceans was derived based on the adjusted river outflow and the estimated contribution from un-monitored areas.

Secondly, we have separately computed annual and monthly continental discharge at each latitude into the oceans by forcing the RTM with the Fekete et al. runoff and the *P-E* fields derived from the NCEP and ECMWF reanalyses with an adjustment for snow effects. These implied discharges were compared with that derived from the stream-flow data.

The new estimate of continental discharge (based on the 921 rivers), together with oceanic *P-E* fluxes derived from the reanalyses and other sources were applied to derive meridional transports of freshwater by the oceans. The main results are summarized as follows:

(1). The use of river mouth outflow increases the global continental discharge by ~18.7% and the total drainage area by ~20.4% compared with estimates using the unadjusted data from the farthest downstream stations (cf. Fig. 1). This result suggests that using unadjusted stream-flow data from the farthest downstream stations (e.g., Perry et al. 1996; Grabs et al. 1996, 2000) substantially underestimates global continental freshwater discharge.

(2). Our 921-river-based estimate of global continental freshwater discharge (excluding Antarctica) is 37288±662 km^3 yr^{-1}, or 1.18±0.02 *Sv*, which is ~7.6% of global *P* and 35% of terrestrial *P*. Although this value is comparable to earlier estimates, large differences exist among the discharges into the individual ocean basins. The estimates of global discharge based on the Fekete et al. runoff and ECMWF *P-E* are slightly higher than the river-based estimate, while the NCEP *P-E* implies lower discharge (Table 3). In general, the reanalysis *P-E* fields underestimate discharge from East Asia and northern Africa (Fig. 3). About 57% of the global discharge comes from the world's 50 largest rivers (Table 2).

(3). When forced with the Fekete et al. runoff and reanalysis *P-E* fields, the RTM simulates the station stream-flow rates reasonably well for world's major rivers (Table 2 and Fig. 4). This is especially true for the Fekete et al. runoff case and suggests that river transport models at 0.5^o resolution, such as the one used in the NCAR CCSM, can realistically simulate the world river system and its routing of terrestrial runoff into the oceans.

(4). The continental discharges into the oceans within each 1^o latitude band implied by the Fekete et al. runoff and reanalysis *P-E* fields agree reasonably well with the river-based estimates, which we regard as the closest to the truth. This is particularly true for the Fekete et al. runoff and ECMWF *P-E* cases and for the global oceans and the Atlantic Ocean (Fig. 4). In general, the NCEP *P-E* underestimates continental discharge at many latitudes for all the ocean basins except for the Arctic Ocean.

(5). The latitudinal distribution of accumulative discharge into the global oceans estimated based on the 921-rivers is similar to that from BR75, although the discharge at individual latitudes differs greatly. The BR75 estimate is unrealistically smooth (Fig. 4) even compared with our 5^o smoothed discharge. Our continental discharge has realistic latitudinal distributions that are needed for reliable estimates of meridional transport of freshwater in the oceans. Earlier estimates (e.g., Wijffels et al. 1992; Wijffels 2001) may contain significant errors as a result of using the unrealistic latitudinal distribution of continental discharge from BR75.

(6). Discharge from most of the world's largest rivers has large annual cycles. For example, the Amazon peaks in May-June, Orinoco peaks in August, Changjiang peaks around July; whereas large Russian rivers (e.g., Yenisey, Lena, Ob,) have a sharp peak in June arising from snow-melt (Fig.2). Basin-wide-integrated precipitation usually does not have the same seasonal phase as for river discharge, which illustrates the important effects of snow accumulation and melt and river transport. The total discharge into the Arctic, the Pacific, and global oceans peaks in June, whereas the peak is in May for the Atlantic Ocean and in August for the Indian Ocean (Fig. 5). Snow accumulation and melt have large effects on the annual cycle of discharge into the Arctic, Atlantic, Pacific, and global oceans, but little influence on the discharge into the Indian Ocean and the Mediterranean and Black Seas.

(7). Our estimates of oceanic freshwater transports (based on the ECMWF *P-E* and the 921-river based discharge) show improved agreement with available direct estimates within the individual ocean basins, especially at southern latitudes. Compared with earlier estimates such as those of Wijffels et al. (1992), our new estimates have considerably higher southward transports in the Atlantic Ocean and higher northward transport in the South Pacific. The transports by the ACC is also higher in our estimates at most longitudes.

The long-term mean values of river runoff and continental discharge reported here is available for free download from NCAR's Climate Analysis Section catalog http://www.cgd.ucar.edu/cas/catalog/.

Acknowledgments: This research was sponsored by grants from NOAA Office of Global Programs and jointly by NOAA/NASA under NOAA grant NA17GP1376.

References

Baumgartner, A. and E. Reichel, 1975: *The World Water Balance.* Elsevier Scientific Publ. Co., New York, 179pp.+ 31 maps.

Blackmon, M. and 25 co-authors, Blackmon, M., et al. 2001: The Community Climate System Model. *Bull. Amer. Meteor. Soc.,* **82**, 2357-2376.

Bodo, B. A., 2001: Annotations for monthly discharge data for world rivers (excluding former Soviet Union), 85 pp. [Available on-line from http://dss.ucar.edu/datasets/ds552.1/docs/]

Branstetter, M. L. and J. S. Famiglietti, 1999: Testing the sensitivity of GCM-simulated runoff to climate model resolution using a parallel river transport algorithm. In: *Proc. 14th Conf. Hydrol.*, Amer. Meteorol. Soc., Jan. 10-15, Dallas, Texas, pp. 391-392.

Branstetter, M. L, 2001: Development of a parallel river transport algorithm and applications to climate studies, Ph.D. dissertation, Dept. of Geological Sci., The Univ. of Texas, Austin, 119pp.

Dai, A., and K. E. Trenberth, 2003: Estimates of freshwater discharge from continents: Latitudinal and seasonal variations. *J. Hydrometeorol.*, in press. [Available from http://www.cgd.ucar.edu/cas/adai/publication-dai.html]

Dai, A., G.A. Meehl, W.M. Washington, T.M.L Wigley, and Julie A. Arblaster, 2001a: Ensemble simulation of 21st century climate changes: business as usual vs. CO_2 stabilization. *Bull. Amer. Meteor. Soc.*, **82**, 2377-2388.

Dai, A., T.M.L. Wigley, G.A. Meehl, and W.M. Washington, 2001b: Effects of stabilizing atmospheric CO_2 on global climate in the next two centuries. *Geophys. Res. Lett.*, **28**, 4511-4514.

da Silva, A. M., C. Young, and S. Levitus, 1994: Atlas of surface marine data. Volume 1: Algorithms and procedures. *NOAA Atlas NESDIS* 6, 83 pp.

Fekete, B.M., C.J. Vörösmarty, and W. Grabs, 2000: Global composite runoff fields based on observed river discharge and simulated water balances. Global Runoff Data Centre (GRDC) Rep. No. 22, Germany, 39 pp. + annex 77 pp. [Available from http://www.bafg.de/grdc.htm]

Fekete, B. M. and C. J. Vörösmarty, C. J. and Grabs, W., 2002: High resolution fields of global runoff combining observed river discharge and simulated water balances, *Global Biogeochem. Cycles*, in press.

Grabs, W.E., T. de Couet, and J. Pauler, 1996: Freshwater fluxes from continents into the world oceans based on data of the global runoff data base. Global Runoff Data Centre (GRDC) Rep. No. 10, Germany, 49 pp. + annex 179 pp. [Available from GRDC, Fed. Inst. of Hydrology, Kaiserin-Augusta-Anlagen 15-17, D-56068 Koblenz, Germany]

Grabs, W.E., F. Portmann, and T. de Couet, 2000: Discharge observation networks in Arctic regions: Computation of the river runoff into the Arctic Ocean, its seasonality and variability. In: *The Freshwater Budget of the Arctic Ocean*, Lewis, E.L. et al. (eds.), Kluwer Academic Publ., Dordrecht, pp. 249-267.

Huffman, G.J., R.F. Adler, P. Arkin, A. Chang, R. Ferraro, A. Gruber, J. Janowiak, A. McNab, B. Rudolf, U. Schneider, 1997: The Global Precipitation Climatology Project (GPCP) combined precipitation data set. *Bull. Amer. Meteor. Soc.*, **78**, 5-20

Josey, S. A., E. C. Kent, and P. K. Taylor, 1998: The Southampton Oceanography Centre (SOC) ocean-atmosphere heat, momentum and freshwater flux atlas. SOC Report No. 6, 30 pp. + 13 pages of figures. [Available from www.soc.soton.ac.uk]

Korzun, V. I., A. A. Sokolov, M. I. Budyko, K. P. Voskrensensky, G. P. Kalinin, A. A. Konoplyantsev, E. S. Korotkevich, and M. I. Lvovich, 1977: Atlas of the world water balance. UNESCO, Paris, 36 pp. + 65 maps.

Lvovich, M. I., 1970: World water balance (general report). In: *World water balance: Proc. Reading Symp.*, July 1970, IASH-UNESCO-WMO Publ. 93, Gentburge-Paris-Geneva, pp. 401-415.

Marcinek, J., 1964: The river discharge from land surface over the globe and its distribution in 5^o zones (in German). Mitt. Inst. Wassserwirtsch Heft 21, Berlin, Germany, 204 pp.

New, M., M. Hulme, and P. Jones, 2000: Representing twentieth-century space-time climate variability. Part I: Developement of a 1961-90 mean monthly terrestrial climatology. *J. Climate,* **12**, 829-856.

Pardaens, A. K., H. T. Banks, J. M. Gregory, and P. R. Rowntree, 2002: Freshwater transport in HadCM3. *Climate Dyn.*}, in press.

Perry, G. D., P. B. Duffy and N. L. Miller, 1996: An extended data set of river discharges for validation of general circulation models. *J. Geophys. Res.*, **101**, 21339-21349.

Probst, J. L. and Y. Tardy, 1987: Long-range streamflow and world continental runoff fluctuations since the begining of this century. *J. Hydrology*, **94**, 289-311.

Trenberth, K. E., and C. J. Guillemot, 1998: Evaluation of the atmospheric moisture and hydrological cycle in the NCEP/NCAR reanalyses. *Clim. Dyn.*, **14**, 213-231.

Trenberth, K. E., J. M. Caron and D. P. Stepaniak, 2001a: The atmospheric energy budget and implications for surface fluxes and ocean heat transports. *Clim. Dyn.*, **17**, 259-276.

Trenberth, K. E., D. P. Stepaniak, J. W. Hurrell and M. Fiorino, 2001b: Quality of reanalyses in the tropics. *J. Climate*, **14**, 1499-1510.

Vörösmarty, C. J., B. M. Fekete, M. Meybeck, R. B. Lammers, 2000: Global system of rivers: Its role in organizing continental land mass and defining land-to-ocean linkages. *Global Biogeochem. Cycles*, **14**, 599-621.

Wijffels, S. E., R. W. Schmitt, H. L. Bryden, and A. Stigebrandt, 1992: Transport of freshwater by the oceans. *J. Phys. Oceanogr.*, **22**, 155-162.

Wijffels, S. E., 2001: Ocean transport of fresh water. In: *Ocean Circulation and Climate*, G. Siedler, J. Church, and J. Gould (eds.), Academic Press, San Diego, 475-488.

Xie, P. and P. A. Arkin, 1997: Global precipitation: A 17 year monthly analysis based on gauge observations, satellite estimates and numerical model outputs, *Bull. Amer. Meteor. Soc.*, **78**, 2539-2558.